Targeting lysine acetylation in inflammatory lung diseases

van den Bosch, Thea

Chapter 4

A novel histone acetyltransferase inhibitor attenuates histone acetylation and inflammatory gene expression in model systems for inflammatory airway diseases

Thea van den Bosch[a], Hannah Wapenaar [a], Niek G. J. Leus[a], Petra E. van der Wouden[a], Jos Hermans[b], Rainer Bischoff[b], Hidde J. Haisma[a], Frank J. Dekker[a]

[a]Department of Chemical and Pharmaceutical Biology, Groningen Research Institute of Pharmacy (GRIP), University of Groningen, The Netherlands
[b]Department of Analytical Biochemistry, Groningen Research Institute of Pharmacy (GRIP), University of Groningen, The Netherlands

Abstract

Inflammatory airway diseases such as asthma and COPD affect millions of people world-wide. Currently, glucocorticoids are being used in the treatment of these diseases, however, not all patients are responsive to this therapy. Therefore, alternative therapeutic strategies are urgently needed. Studying the underlying biological processes may give rise to novel therapeutic targets. Some of these processes may include epigenetic regulation, such as regulation by lysine acetylation. Lysine acetylations are installed by histone acetyltransferases (HATs) and removed by histone deacetylases (HDACs). Observations that asthma and chronic obstructive pulmonary disease are characterized by increased HAT activity and reduced HDAC activity, indicate that HAT inhibitors (HATi) could be starting points for new therapies for these diseases, based on their potential to restore the balance between HAT and HDAC activities. Development of HATi is a challenge which was addressed with limited success so far. Recently, 4-amino-1-naphtol was discovered at our lab to be a non-selective inhibitor for the HATs p300 (KAT3B), MOF (KAT8) and PCAF (KAT2B). In this study, we focused on the characterization of the effects of 4-amino-1-naphtol in murine macrophages and precision-cut lung slices as model systems for inflammatory lung diseases, where it demonstrated inhibition of both histone acetylation and pro-inflammatory gene expression. This suggests that the concept of HAT inhibition, as a basis for novel therapies for inflammatory airway diseases such as asthma and COPD, is promising.

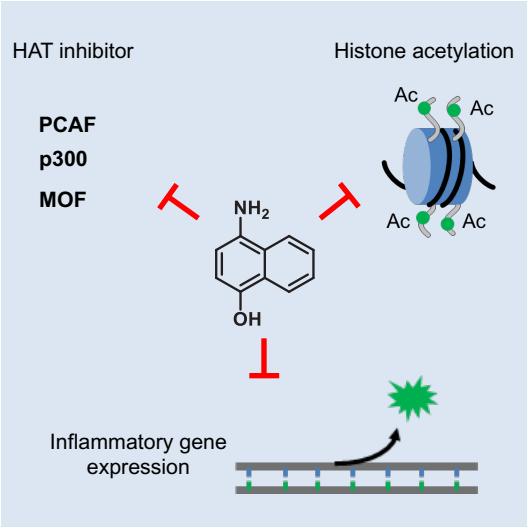

Introduction

Chronic inflammatory diseases of the lung, such as asthma or chronic obstructive pulmonary disease (COPD), are a major social and economic burden for society. Currently, corticosteroids are the standard treatment for these diseases. However, there is an unmet need for new treatments since severe asthmatics display glucocorticoid resistance (1). Next to this, the effectivity of glucocorticoids in COPD patients is subject to debate (2)(3). Discovery of novel therapeutic targets is necessary, since this can aid in the development of novel therapies to meet the medical needs of this group of patients. Such novel targets can be found by studying biological processes underlying these diseases.

Some of these processes may be the epigenetic modification of chromatin structure. Epigenetics is defined as the structural adaptation of chromosomal regions so as to register, signal or perpetuate altered transcriptional activity (4). Epigenetics is a field of study in which novel therapeutic targets are found for various diseases, such as inflammatory diseases and cancer (5). Epigenetic processes include post-translational modifications of histones such as lysine acetylations. Lysine acetylations of histones play an important role in the regulation of gene transcription by controlling the chromatin structure of DNA (6). These lysine acetylations are installed by histone acetyltransferases (HATs) and removed by histone deacetylases (HDACs). These enzymes balance lysine acetylation, resulting in a controlled expression of genes. A disturbance of this balance can result in disease states.

Asthma, for example, is characterized by increased HAT activity (7). There is increased HAT activity, and decreased HDAC activity and HDAC1 and HDAC2 expression, in bronchial biopsies and bronchoalveolar lavage macrophages obtained from asthmatics compared to healthy adults (8) (9), thereby shifting the balance towards HAT activity. Also, HAT activity was found to be increased in peripheral blood mononuclear cells (PBMCs) obtained from mild and severe asthmatic children compared to healthy children, whereas HDAC activity was decreased (10). Furthermore, in isolated PBMCs from patients with neutrophilic asthma, there was increased HAT and decreased HDAC activity (11). More recently, it was found that acetylation of histone H3 lysine 18 (H3K18) is elevated in epithelium from asthmatics compared to healthy subjects (12), which is in line with a shift towards increased HAT activity. Next to this, COPD is characterized by a loss of SIRT1 (13), and HDAC2 expression and activity (14) (7). Also, decreased HDAC2 expression was found in PBMCs and lymphocytes in COPD (15) (16). Altogether, both asthma and COPD are characterized by increased HAT and decreased HDAC activity. This indicates that these enzymes represent potential drug targets in these diseases (17) (18). Restoring the balance between HAT and HDAC activity using small molecule HAT inhibitors (HATi) could be an alternative therapeutic strategy for these inflammatory airway diseases.

Development of HATi is an important challenge that has been addressed with limited success so far. The HATs are a disparate group of enzymes from which most isoenzymes can

be assigned to five main families based on primary structure homology. Three families that have been studied extensively are the GNAT (GCN5-related N-acetyltransferase) family, the p300/CBP (p300/CREB binding protein) family and the MYST (acronym for MOZ, Ybf2, Sas2, and Tip60) family (19). At our lab, 4-amino-1-naphtol (referred to as compound **13**) was recently discovered to potently inhibit p300 (also known as KAT3B), MOF (also known as KAT8) and PCAF (also known KAT2B) (Table 1).

Here, biological studies were performed to investigate the effects of the HATi **13** in model systems for inflammatory airway diseases such as asthma and COPD. As model systems both RAW264.7 murine macrophages as well as murine precision-cut lung slices (PCLS) were selected, which were treated with LPS and IFNγ as an inflammatory stimulus. Here we demonstrate that **13** inhibits histone acetylation as well as pro-inflammatory gene expression in these model systems. This suggests that the concept of HAT inhibition as a basis for novel therapies for inflammatory airway diseases is promising.

4 Results and Discussion

Effect on histone acetylation in RAW264.7 murine macrophages

After discovering **13** (Table 1) as a potent HATi at our lab, cellular assays were done to investigate whether the inhibition of recombinant HATs by **13** correlates with inhibition of histone acetylation in cells. Due to its phenolic structure, **13** has anti-oxidant activity. Since the anti-oxidant activity of **13** could result in effects unrelated to the HAT inhibition, **9** (Table 1) was applied in cellular assays as an anti-oxidant control for **13** to provide a reference for whether the observed cellular effects of **13** could be attributed to its anti-oxidant activity. Compound **9** was selected as a control because it is structurally very similar to **13**, and also shows similar anti-oxidant activity (data not shown), but does not show HAT inhibitory activity. First, the viability of **13** treated RAW264.7 cells was tested using an MTS assay. Concentrations up to and including 1.5 μM did not significantly change viability (Fig. S1A). At 3 μM, there was a reduction in viability of 18% compared to untreated RAW264.7 cells (Fig. S1A). The control compound **9** did not change cell viability (Fig. S1B), indicating that effects on cell viability of **13** could be due to HAT inhibition. To study whether **13** influenced histone acetylation status, RAW264.7 cells were incubated with **13** at 0.375, 0.75, 1.5 or 3 μM. Both a long (20 hours) and short (6 hours) incubation time was studied in order to be able to monitor both early and late onset effects of **13**. Higher concentrations of **13** were not studied due to further decreased viability of RAW264.7 cells. After incubation with **13**, histones were extracted and analyzed for acetylation using Western blot. Using an anti-pan-Ac-lysine antibody, dose-dependent reductions in histone acetylation were observed at all studied concentrations of **13** at 20 hrs but not at 6 hrs of incubation (Fig. 1A). Analysis of pixel density of the bands indicated a dose-dependent reduction in histone acetylation at 20

hrs, which became significant at 3 μM for histone H3, and at 0.75 μM for histone H4 (Figs. 1B and C). Taken together, this indicates that upon treatment with **13**, there is inhibition of histone acetylation, with some selectivity in terms of which histones are affected. Treatment with **9** did not affect histone acetylation under these conditions (Figs. 2A-D), which is consistent with the hypothesis that the reduction of histone acetylation seen with **13** was not due to its anti-oxidant properties.

Table 1. IC_{50} values of compound **13** and compound **9** on PCAF, p300 and MOF.

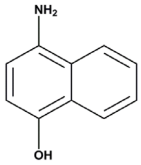

13

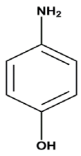

9

Compound	IC_{50} p300 (μM)	IC_{50} MOF (μM)	IC_{50} PCAF (μM)
13	1.4 ± 0.1	9.6 ± 3.0	3.6 ± 1.1
9	> 500	> 500	> 500

Since effects were observed at 20 but not at 6 hrs of incubation with **13**, we continued our cell based studies with the 20 hrs incubation time point only. To study in more detail which parts of the histone H3 and H4 sequence are affected upon **13** treatment, a mass spectrometry based technique was employed as previously described (20). Reduced acetylation status was found on two peptides from histone H3 (H3 9-17 containing K9 and K14, and H3 18-26 containing K18 and K23) (Figs. 3A and B) at 3 μM **13** after 20 hrs of incubation. One peptide from histone H4 had reduced acetylation status upon **13** treatment (H4 4-17 containing K5, K8, K12 and K16) (Fig. 3C), which was significant at all studied concentrations. No changes in acetylation status were detected on other histone peptides (data not shown). This indicates that **13** affects acetylation of the N-terminal tails of histones H3 and H4, and confirms that it affects H4 at a lower concentration than H3, which is in line with the anti-pan-Ac-lysine antibody western blot results. Differences in the extent of inhibition of the different HATs by **13**, in relation to the target lysines of these HATs, could explain this. Furthermore, **9** did not affect histone acetylation in this mass spectrometry analysis under the same conditions (Figs. 2E-F). Altogether, treatment with **13** gives rise to pronounced inhibition of histone acetylation in RAW264.7 macrophages.

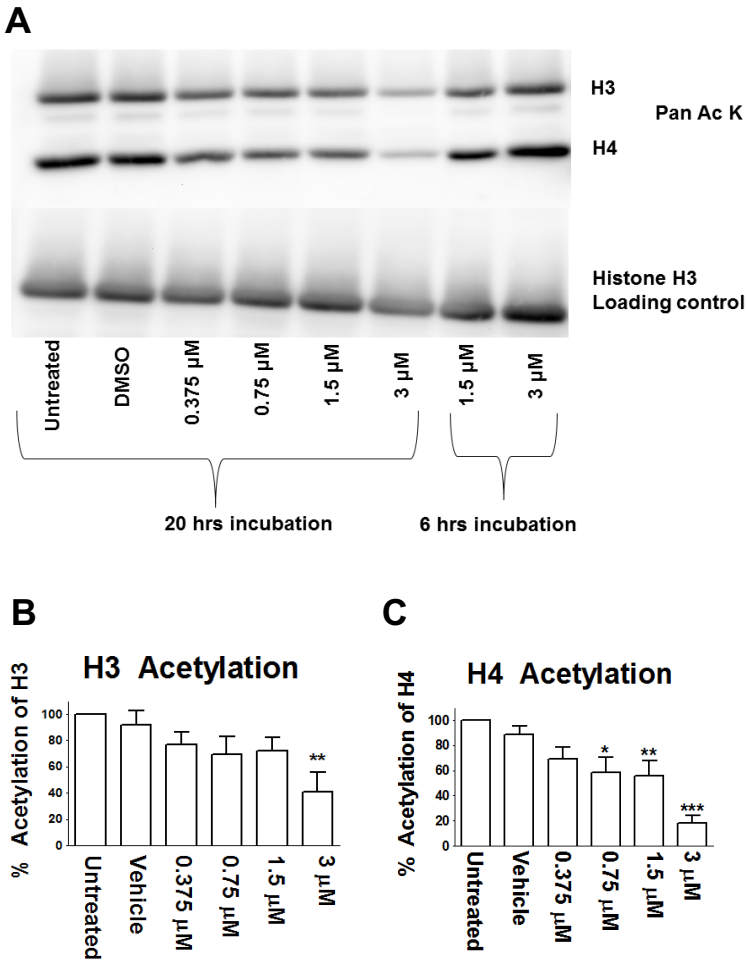

Figure 1. Compound 13 dose dependently reduces histone acetylation in RAW264.7 murine macrophages after 20 hrs of incubation, but not after 6 hrs of incubation. RAW264.7 cells were incubated with **13** at the indicated concentrations for 20 hrs, after which histones were extracted. Histones were resolved by SDS PAGE and immunoblotted for pan-acetylated lysine, or histone H3 as loading control. A) Western blot representative image of 3 independent experiments. The western blot image was cropped to show only the histones. Densitometry results are also shown of 3-6 independent experiments for histone as percentage of acetylation of H3 (B) and H4 (C) compared to untreated (set as 100%).

Effect on SAHA-induced histone hyperacetylation in murine precision-cut lung slices

We moved on to a model system more closely resembling the *in-vivo* situation, i.e. murine precision-cut lung slices (PCLS), which were subjected to LPS and IFNγ as an inflammatory stimulus. This can be used as an *ex-vivo* model system for lung tissue inflammation. Lung tissue structure and cell-cell interactions are maintained in PCLS (21), which is not the case

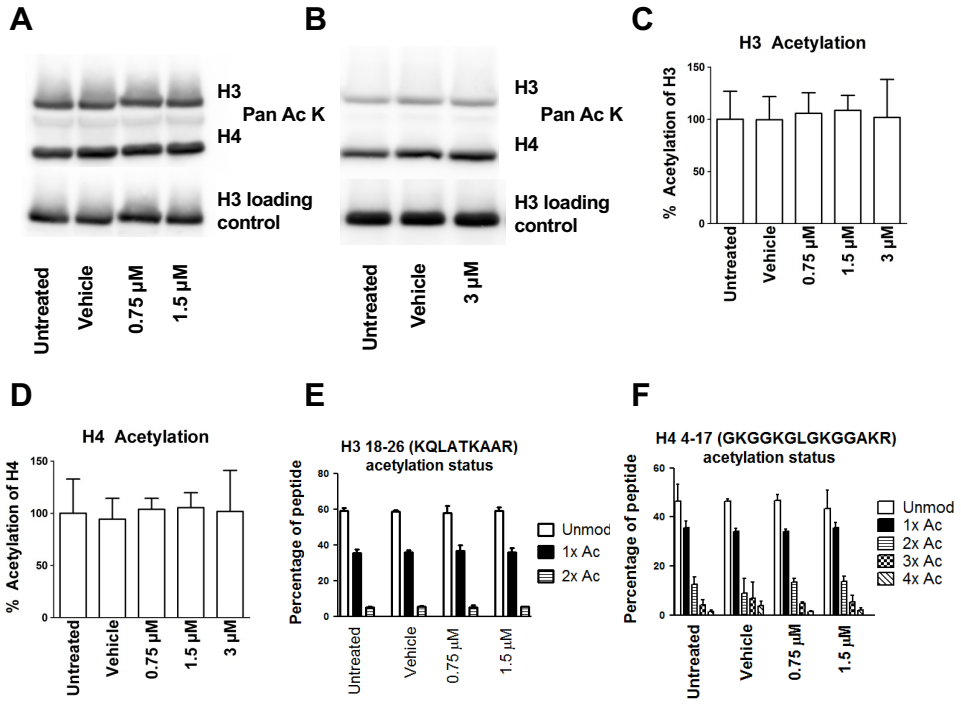

Figure 2. A) and B) No effect of the control compound **9** on histone acetylation in RAW264.7 cells after 20 hours treatment. Western blot representative images of 3 independent experiments. The western blot images were cropped to show only the histones. C) and D) Densitometry results are also shown of 3-6 independent experiments as percentage of acetylation of H3 and H4 compared to untreated (set as 100%). E) and F) Mass spectrometry results are shown on the peptides H3 res. 18-26 and of H4 res. 4-17. Data are presented as mean values ± SD of 3 independent experiments.

in cell cultures. An additional advantage of the use of tissue slices is that it reduces the need for experimental animals (22). We studied the effects of **13** on histone acetylation in PCLS. First, the viability of PCLS treated with **13** was studied by lactate dehydrogenase (LDH) assay (Fig. S2A). Concentrations of **13** at 2, 5, 7.5 or 10 µM were selected for treatment of PCLS. No significant changes were observed, except at 10 µM of **13**, where LDH release was increased by 12% (Fig. S2A). Compound **9** did not give rise to changes in LDH release of PCLS (Fig. S2B), which could again suggest target-dependent viability changes. Then, PCLS were treated with **13** at 2, 5, 7.5 or 10 µM, histones were extracted and acetylation status was studied using mass spectrometry. No significant inhibition of histone acetylation was observed upon treatment of PCLS with **13** at these concentrations (Fig. 4A). PCLS were then subjected to a co-treatment of **13** with the non-selective HDAC inhibitor suberoylanilide hydroxamic acid (SAHA). For previously described HATi, co-treatments with an HDACi are oftentimes necessary to reveal or enlarge effects on histone acetylation. For example,

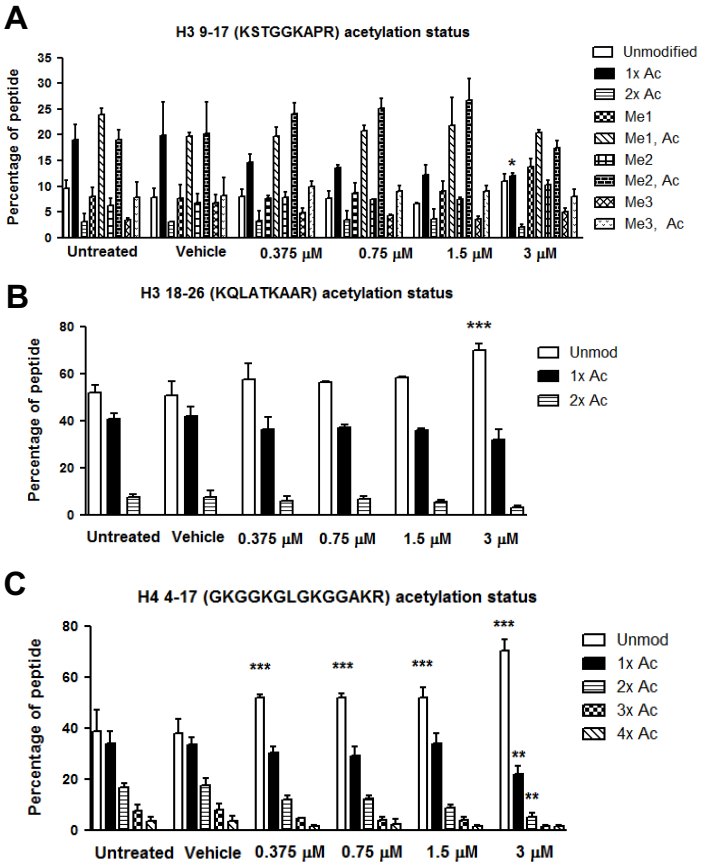

Figure 3. Selectivity on N-terminal tails of H4 and H3 upon 13 treatment in RAW264.7 murine macrophages. RAW264.7 cells were incubated with **13** at the indicated concentrations for 20 hrs, after which histones were extracted. Histones were resolved by SDS PAGE, and histones H3 and H4 were excised from the gels. Gel pieces were treated with acetic anhydride d6, followed by trypsin digestion. Resulting peptides were subjected to LC-MS/MS analysis. Compound **13** dose dependently reduces histone acetylation in RAW264.7 murine macrophages after 20 hrs of incubation of histone A) H3 res. 9-17 B) H3 res. 18-26 C) H4 res. 4-17. Data are presented as mean values ± SD of 3 independent experiments. *** $p < 0.001$, ** $p < 0.01$ and * $p < 0.05$ compared to vehicle (DMSO treated) cells. No significant differences were observed between control and vehicle treated cells.

this was shown for a derivative of the non-selective HATi anacardic acid MG149 in the cell lines MOPL8 and K562 (23). SAHA increased histone acetylation in PCLS (Fig. 4B). Importantly, upon addition of **13**, inhibition of histone acetylation was observed compared to SAHA treatment on histone H4 res. 4-17 (Fig. 5A). This effect was dose-dependent and became significant at 10 µM **13**. Furthermore, **9** at 10 µM in combination with SAHA did not demonstrate this effect (Fig. 4B), consistent with the hypothesis that the reduction

of histone acetylation seen by **13** was not due to its anti-oxidant properties. On all other studied peptides from histone H4 and histone H3, no increase in acetylation was observed upon SAHA treatment, and there was also no effect of **13** in co-treatment on these peptides (data not shown).

In contrast to RAW264.7 macrophages, a co-treatment with SAHA was necessary in PCLS to reveal inhibition of histone acetylation by **13**. This could be explained by the fact that many different cell types are present in PCLS. Whereas pronounced effects were observed in RAW264.7 macrophages, in cell types other than macrophages, effects upon **13** treatment on histone acetylation may be less. This could be due to different reasons. There could be a difference in the balance between HAT and HDAC activities between RAW264.7 and individual cell types in PCLS. For example, differences in glycolysis rates and Ac-CoA levels between RAW264.7 and individual cell types in PCLS may be possible, and this has been described to affect histone acetylation and HAT activities (24), and therefore could explain differences in effects upon HAT inhibition between RAW264.7 and PCLS. Also, rates of acetylation turnover on histone lysines as described in (25) may be different between the different cell types. Interestingly, it was demonstrated that the HDACi butyrate upregulates acetylations only on lysines with high turnover, suggesting that the turnover of acetylation of a particular lysine is one aspect which dictates whether that lysine is responsive to HDACi treatment (25), which may also be an important aspect to consider upon treatments with HATi. Therefore, differences in acetylation turnover between RAW264.7 and individual cell types in PCLS may also explain the need for SAHA co-treatment to observe effect of **13** on histone acetylation. Taken together, the reduction of histone acetylation observed in both the RAW264.7 macrophages and the PCLS are consistent with the hypothesis that the inhibition of recombinant HATs by **13** correlates with inhibition of histone acetylation in the cells and PCLS; and the fact that **9** does not show these effects is consistent with the hypothesis that the observed effects of **13** were not due to its anti-oxidant properties.

Effect on pro-inflammatory gene expression in RAW264.7 murine macrophages and murine precision-cut lung slices

To investigate whether the inhibition of histone acetylation by **13** correlates with inhibition of pro-inflammatory gene expression, mRNA levels of the pro-inflammatory genes *TNFα*, *iNOS*, *IL1β*, *IL6*, and *KC* (murine *IL8*) were monitored using RT-q-PCR in both RAW264.7 macrophages and PCLS. An LPS and IFNγ stimulus (at 10 ng/mL of each) induced expression of these pro-inflammatory genes in RAW264.7 macrophages. Small (but some significant) changes in gene expression were observed upon **13** incubation before receiving this stimulus (Fig. S3A-E). Exposure of PCLS to the same LPS and IFNγ stimulus upregulated mRNA expression levels of the pro-inflammatory genes, with the exception of *KC*, which was not affected by the stimulus (Figs. 5B-G). Upon **13** treatment before receiving the stimulus, dose-dependent reductions in the LPS and IFNγ-induced gene expression

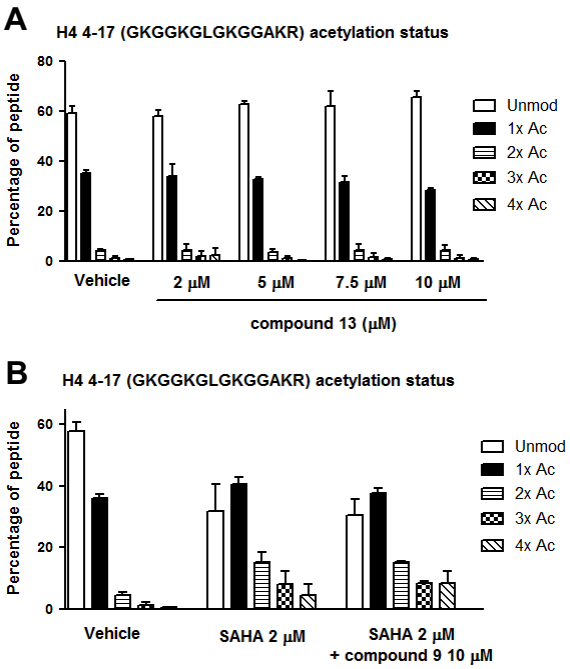

Figure 4. (A) No effect of **13** on histone acetylation on H4 res. 4-17 in PCLS without SAHA co-treatment. Data are presented as mean values ± SD of 2 independent experiments. (B) In PCLS, the control compound **9** at 10 µM in combination with 2 µM SAHA did not demonstrate inhibition of histone acetylation on H4 res. 4-17 in combination with SAHA compared to SAHA treatment alone. Data are presented as mean values ± SD of 3 independent experiments.

levels of *TNFα*, *iNOS*, *IL1β*, *IL12b* and *IL6* were observed (Figs. 5B-F). The expression of *KC* was not significantly changed upon **13** treatment (Fig. 5G). In addition to pro-inflammatory genes, the expression of the anti-inflammatory gene *IL10* was monitored, however, no significant changes were observed (Fig. 5H). Compound **9** did not affect gene expression in PCLS (Figs. 6A-G) consistent with the hypothesis that the reduction in pro-inflammatory gene expression seen by **13** was not due to its anti-oxidant properties. Taken together this indicates that **13** gives rise to large reductions in pro-inflammatory gene expression in PCLS stimulated with LPS and IFNγ.

Considering the roles in pro-inflammatory gene expression that have been described for the HATs which are inhibited by **13**, these observed effects could be in line with literature. For example, p300 and PCAF have been described to regulate the NF-κB transcription factor by affecting its acetylation status, by which they influence pro-inflammatory gene expression (26). Since the effects of **13** in RAW264.7 macrophages on gene expression were much less pronounced compared to the effects in PCLS, it could be that effects of **13** on gene expression in cell types other than macrophages present in PCLS are more pronounced, or

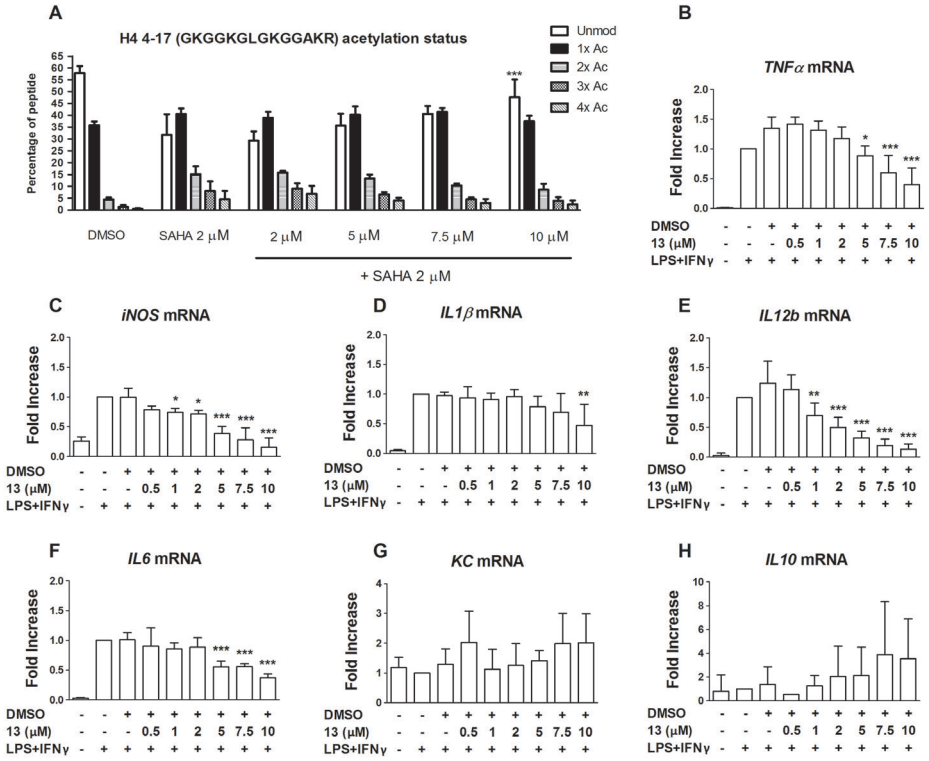

Figure 5. A) Compound **13** dose dependently reduces histone acetylation of H4 res. 4-17 in PCLS after 20 hrs of incubation in combination with SAHA compared to SAHA treatment alone. PCLS were incubated with **13** at the indicated concentrations for 20 hrs, in combination with 2 μM SAHA. For the last 4 hrs of the experiment, PCLS were incubated with LPS and IFNγ (10 ng/mL of each) in continued presence of the inhibitors. Histones were then extracted. Histones were resolved by SDS PAGE, and histones H3 and H4 were excised from the gels. Gel pieces were treated with acetic anhydride-d6, followed by trypsin digestion. Resulting peptides were subjected to LC-MS/MS analysis. Data are presented as mean values ± SD of 3 independent experiments. No significant differences were detected between vehicle treated PCLS and untreated or LPS IFNγ treated PCLS. B-H) Compound **13** dose dependently reduces pro-inflammatory gene expression of B) *TNFα* C) *iNOS* D) *IL1β* E) *IL12b*, and F) *IL6* in murine precision-cut lung slices (PCLS). No significant changes were observed on the expression of G) *KC* or H) *IL10*. PCLS were pre-treated with **13** at the indicated concentrations for 16 hours, after which an inflammatory LPS and IFNγ stimulus (10 ng/mL of each) was given for 4 hours in continued presence of the inhibitor (making the total incubation time with the inhibitor 20 hrs). Subsequently, gene expression was analyzed by RT-q-PCR. For vehicle treatment, PCLS were pre-treated with the inhibitor solvent DMSO. Data represent the target gene expression normalized to the reference gene. The values shown are means ± SD of 2-4 independent experiments. *** $p < 0.001$, ** $p < 0.01$ and * $p < 0.05$ compared to vehicle.

that perhaps the interactions between different cell types in PCLS are important, and that **13** affects these interactions. Further studies need to be done to investigate whether the inhibition of histone acetylation upon **13** treatment can be directly linked to reductions in gene expression in a causative manner. Also, the observed biological effects are most

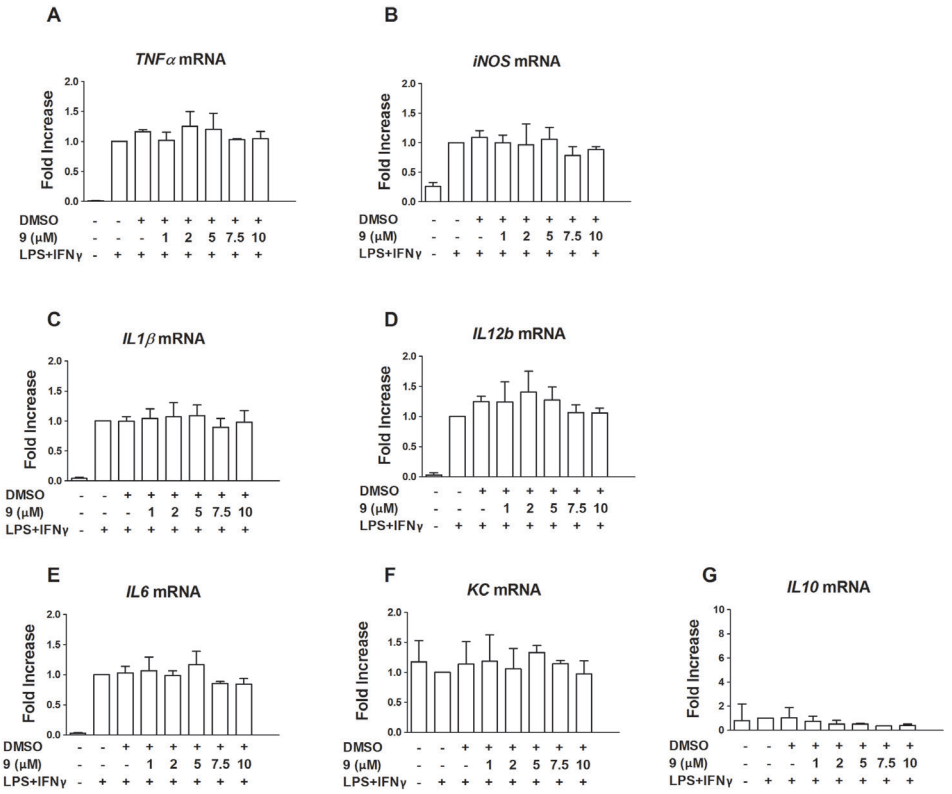

Figure 6. The control compound **9** in PCLS does not affect expression of A) *TNFα*, B) *iNOS*, C) *IL1β*, D) *IL12b*, E) *IL6*, F) *KC*, and G) *IL10*. PCLS were pre-treated with **9** at the indicated concentrations for 16 hours, after which an inflammatory LPS and IFNγ stimulus (10 ng/mL of each) was given for 4 hours in continued presence of the inhibitor (making the total incubation time with the inhibitor 20 hrs). Subsequently, gene expression was analyzed by RT-q-PCR. For vehicle treatment, PCLS were pre-treated with the inhibitor solvent DMSO. Data represent the target gene expression normalized to the reference gene. The values shown are means ± SD of 3 independent experiments.

likely the result of inhibition of multiple HATs, and further study is required to discern the roles and contributions of the individual isoenzymes. Nevertheless, the reductions in pro-inflammatory gene expression in PCLS upon **13** treatment suggest that the concept of HAT inhibition in the treatment of inflammatory lung diseases is promising.

Concluding remarks

In biological studies, **13** inhibited histone acetylation in RAW264.7 macrophages and PCLS. Next to this, promising reductions in pro-inflammatory gene expression upon **13** treatment were observed in PCLS stimulated with LPS and IFNγ as models of inflammation. Thus, **13** has been identified as a compound that inhibits recombinant HATs, and histone acetylation as well as pro-inflammatory gene expression in model systems for inflammatory lung diseases. This study suggests that the concept of HAT inhibition in the development of novel treatments for inflammatory lung diseases is promising.

Experimental Section

General Reagents and Materials

All chemicals and reagents were purchased from Sigma Aldrich (St. Louis, Missouri, USA) unless otherwise stated. Suberoylanilide hydroxamic acid (SAHA) was purchased from Selleckchem (Huissen, The Netherlands). The purity of SAHA was assessed by HPLC, MS, and NMR by Selleckchem and was > 99%.

RAW264.7 cell culture

For the RAW264.7 murine macrophages, cell culture was carried out as described previously (20). Mouse RAW 264.7 macrophages were obtained from the American Type Culture Collection (ATCC; Wesel, Germany) and cultured in plastic tissue culture plates or flasks (Costar Europe, Badhoevedorp, The Netherlands) at 37 °C under 5% CO_2/95% air in Dulbecco's Modification of Eagle's Medium (DMEM) containing GlutaMAX™ (Gibco® by Life Technologies, Bleiswijk, The Netherlands) supplemented with 10% (v/v) heat inactivated fetal bovine serum (FBS; Invitrogen, Breda, The Netherlands), 2 mM additional GlutaMAX™ (Gibco® by Life Technologies), 100 U/ml penicillin (Gibco® by Life Technologies) and 100 µg/ml streptomycin (Gibco® by Life Technologies). RAW 264.7 macrophages were used between passage 5 and 20.

Western blot and antibodies

To study histone acetylation, 7 µg of extracted histones were loaded on a 15% polyacrylamide gel, resolved by sodium dodecyl sulfate polyacrylamide gel electrophoresis (SDS-PAGE) and electroblotted to PVDF membranes. The membranes were incubated with anti-acetyl lysine antibody (Millipore AB3879), or with anti-histone H3 antibody (Cell Signalling 4499), followed by a swine anti-rabbit HRP conjugated antibody (DakoCytomation, P0217). All antibodies were used according to manufacturer instructions. Bands were visualized using a 1B1581 visiglo prime HRP chemiluminescence substrate kit from Amresco (Solon, Ohio,

USA). Bands were scanned using a G:BOX iChemi system from Syngene (Cambridge, UK) and quantified using ImageJ quantification software. The histone H3 signal was used as loading control. The experiments were performed at least in triplicate.

Precision-cut lung slices

PCLS were prepared as previously described for guinea pig (27) with the following modifications. Male mice were anesthetized by a subcutaneous injection of ketamine (75 mg/kg, Alfasan, Woerden, The Netherlands) and dexdomitor (0.5 mg/kg, Orion Pharma, Mechelen, Belgium). Subsequently, the trachea was cannulated, and the animal was exsanguinated by cutting the jugular vein, after which the lungs were filled trough the cannula with 1.5 mL of a low melting-point agarose solution (1.5% final concentration (Gerbu Biotechnik GmbH, Wieblingen, Germany)) in $CaCl_2$ (0.9 mM), $MgSO_4$ (0.4 mM), KCl (2.7 mM), NaCl (58.2 mM), NaH_2PO_4 (0.6 mM), glucose (8.4 mM), $NaHCO_3$ (13 mM), HEPES (12.6 mM, Gibco by Life Technologies, Bleiswijk, The Netherlands), sodium pyruvate (0.5 mM, GE Healthcare Life Sciences, Eindhoven, The Netherlands), glutamine (1 mM, Gibco by Life Technologies), MEM–amino acid mixture (1:50, Gibco by Life Technologies), and MEM–vitamins mixture (1:100, Gibco by Life Technologies), pH 7.2). The lungs were placed on ice for 15 min to solidify the agarose for slicing. The lobes were separated, and tissue cores were prepared of the individual lobes, after which the lobes were sliced at a thickness of 250 μm in medium composed of $CaCl_2$ (1.8 mM), $MgSO_4$ (0.8 mM), KCl (5.4 mM), NaCl (116.4 mM), NaH_2PO_4 (1.2 mM), glucose (16.7 mM), $NaHCO_3$ (26.1 mM), and HEPES (25.2 mM), pH 7.2, using a tissue slicer (Compresstome VF-300 microtome, Precisionary Instruments, San Jose, CA, USA). Tissue slices were incubated at 37 °C in a humid atmosphere under 5% CO_2/95% air. In order to remove the agarose and cell debris from the tissue, slices were washed every 30 min (four times in total) in medium composed of $CaCl_2$ (1.8 mM), $MgSO_4$ (0.8 mM), KCl (5.4 mM), NaCl (116.4 mM), NaH_2PO_4 (1.2 mM), glucose (16.7 mM), $NaHCO_3$ (26.1 mM), HEPES (25.2 mM), sodium pyruvate (1 mM), glutamine (2 mM), MEM–amino acid mixture (1:50), MEM–vitamins mixture (1:100), penicillin (100 U/mL, Gibco by Life Technologies), and streptomycin (100 μg/mL, Gibco by Life Technologies), pH 7.2. Chemicals to prepare the media described above were obtained from Sigma-Aldrich (Zwijndrecht, The Netherlands) unless stated otherwise and were of analytical grade.

PCLS were incubated in Dulbecco's modified Eagle's medium (DMEM, Gibco by Life Technologies) supplemented with sodium pyruvate (1 mM), MEM–nonessential amino acid mixture (1:100, Gibco by Life Technologies), gentamycin (45 μg/mL, Gibco by Life Technologies), penicillin (100 U/mL), streptomycin (100 μg/mL), and amphotericin B (1.5 μg/mL, Gibco by Life Technologies). Slices were cultured at 37 °C in a humidified atmosphere under 5% CO_2/95% air in 12-well tissue culture plates (Costar Europe, Badhoevedorp, The Netherlands), using 3 slices per well. Slices were treated with inhibitors

for 20 hrs. During the last 4 h of the experiments, tissue slices were stimulated with 10 ng/mL lipopolysaccharide (LPS, *Escherichia coli*, serotype 0111:B4; Sigma-Aldrich) and 10 ng/mL interferon gamma (IFNγ, cat. no. 315-05; PeproTech, Hamburg, Germany).

To assess the viability of the PCLS subjected to inhibitors, the amount of lactate dehydrogenase (LDH) released from the tissue slices into the incubation medium was analyzed. Maximal LDH release was determined by lysing 3 slices with 1% Triton X-100 for 30 min at 37 °C at the start of the experiments. Supernatants were stored at −80 °C. LDH release was determined using an assay form Roche Diagnostics (Mannheim, Germany), and was measured using a Hitachi automatic analyzer (Modular Analytics, Roche Diagnostics). LDH release from the PCLS into the incubation medium was plotted relative to maximal LDH release.

All experiments were performed according to national guidelines and upon approval of the experimental procedures by the local Animal Care and Use committee of Groningen University, DEC number 6962A.

Histone extractions

For the histone extractions from PCLS, PCLS were treated with **13** at 2, 5, 7.5 or 10 μM, or with **9** at 10 μM, in single treatments or in combination with 2 μM SAHA. PCLS were incubated with the inhibitors for 16 hrs. Subsequently, PCLS were stimulated with LPS and IFNγ in continued presence of the inhibitors as described above for the gene expression analysis. For the histone extractions from RAW264.7, cells were treated with **13** at 0.375, 0.75, 1.5 or 3 μM, or with **9** at 0.75, 1.5 or 3 μM. The cells were incubated with the inhibitors for 20 hrs.

For the histone extractions, the RAW264.7 macrophages were lysed by sonication for two 15 second intervals at amplitude 40% (using a Vibra-Cell VCX 130 from Sonics & Materials, Newtown USA), in ice-cold Dulbecco's Phosphate-buffered Saline (DPBS; Gibco by Life Technologies) supplemented with protease inhibitors (#88266, Thermo Scientific, Rockford, IL, USA) and sodium butyrate (1 mM final concentration).

PCLS were lysed in the same buffer, using glass beads (1.0 mm diameter Cat. No 11079110, BioSpec Products, Breda, The Netherlands) and a Mini-BeadBeater 24 machine (BioSpec Products, Breda, The Netherlands), for 2-3 cycles of 40 seconds, with 30 seconds of incubation on ice in between the cycles. Samples were then sonicated for 15 seconds with 1 second on and 1 second off intervals at amplitude 40% (using a Vibra-Cell VCX 130 from Sonics & Materials, Newtown USA).

The RAW264.7 or PCLS lysates were then centrifuged at 10,000 × *g* for 10 min. After removing the supernatant, the pellets were washed two times with a Tris-EDTA buffer (pH 8.0, 10 mM and 13 mM respectively). Pellets were collected after centrifugation at 10,000 × *g* for 10 min. Washed pellets were resuspended in 0.4 N H_2SO_4 and incubated on ice for 1 hour with gentle agitation. After centrifugation at 10,000 × *g* for 10 min, the supernatants

were collected. Extracted histones were then precipitated by the addition of acetone, which was incubated overnight at 4 °C. The precipitated histones were resuspended in H_2O.

Acetylation of histones with acetic anhydride-d6 (in-gel) and nano LC-MS/MS QTOF

For the in-gel reactions of histones with acetic anhydride-d6, 7 µg of histones were loaded on a 15% polyacrylamide gel and resolved by sodium dodecyl sulfate polyacrylamide gel electrophoresis (SDS-PAGE). After staining with InstantBlue (product #ISB1 L from Expedeon, Cambridge, UK) bands for histones H3 and H4 were excised from the gel. Then 50 µL of acetonitrile and 50 µL of ammonium bicarbonate buffer (100 mM) were added to destain the gel bands. Gel bands were dried in acetonitrile. Subsequently, 5 µL of acetic anhydride-d6 was added, after which 100 µL of ammonium bicarbonate (1 M) was added immediately. Subsequently, samples were incubated at 37 °C for 15 min. Gel bands were washed 3 times with H_2O, and the acetic anhydride-d6 reaction was repeated. After the second reaction, gel bands were dried using acetonitrile and trypsin (Promega, Leiden, the Netherlands, # V511A) was added at a 1:20 ratio in ammonium bicarbonate (50 mM). Histones were digested at 37 °C for 16 h. Supernatants containing histone peptides were subjected to LC MS/MS analysis.

For the analysis of acetylation status of the histone peptides by LC-MS/MS a quadruple time-of-flight mass spectrometer (QTOF, Bruker MaxisPlus) with a captive spray ionization interface was coupled to a nanoLC system (Dionex Ultimate3000). The auto sampler was held at 5°C, equipped with a 20 µl injection loop and used in the micro liter pick-up mode. A 300 µm x 5 mm trap column and a 75 µm x 150 mm analytical column both filled with C18 Pepmap 100 (Thermo Scienticic), 5 µm and 3 µm respectively were used for peptide forward flush trapping and separation. The following mobile phases were used for LC separations: solvent A, ultrapure water (resistance 18.2 MΩ, Millipore) with 0.1% (v/v) formic acid (FA), and solvent B, acetonitrile (ACN) with 0.1% (v/v) FA. The samples were injected (10 µl) and trapped for 2 minutes (the trapping time was set to a minimal value to prevent the loss of early eluting peptides) at a flow rate of 10 µL/min in a solution of 1% (v/v) ACN and 0.1% (v/v) FA in ultrapure water. The peptide separation was performed at 0.3 µl/min using a linear gradient from 1-35.5% solvent B in 65 minutes after a 4 min isocratic period at 1%. Hereafter the column was eluted with 90% solvent B for 10 minutes and conditioned with 1% solvent B for another 10 minutes after which it was ready for the next injection. The identification of peptides was based on data collected in auto MS/MS mode (2 GHz) with a maximum of 5 precursors per cycle and an active exclusion of 0.3 min using a mass range of 200-1500 amu, and was done using PEAKS Studio 7.5 (Bioinformatics Solutions Inc., Canada).

Gene expression analysis in PCLS by RT-q-PCR

For gene expression analysis, PCLS were pre-treated with compounds at the indicated concentrations for 16 hrs. Inhibitor stocks were prepared in DMSO and were further diluted in culture medium. Vehicle treatment constituted of pre-treatment with 0.15% DMSO for PCLS, for 16 hrs. Subsequently, PCLS were stimulated with LPS and IFNγ in continued presence of the inhibitors, with 10 ng/mL LPS (*Escherichia coli*, serotype 0111:B4; Sigma-Aldrich) and 10 ng/mL IFNγ (cat.#315-05; PeproTech, Hamburg, Germany) for 4 hrs. Gene expression analysis by RT-q-PCR was performed as described previously (28). The primers were purchased as Assay-on-Demand (Applied Biosystems) and were as follows: for *TNFα* (Mm00443258_m1), *IL1β* (Mm00434228_m1), *IL6* (Mm00446190_m1), *KC* (Mm04208136_m1), *iNOS* (Mm00440502_m1) *IL12b* (Mm00434174_m1), *IL10* (Mm00439614_m1 and Hs00961622_m1), and *GAPDH* (Mm99999915_g1).

Statistical analysis

We used GraphPad Prism 5.0 software (GraphPad Software Inc., San Diego CA, USA) to perform statistical analysis for all histone acetylation and gene expression experiments. Data are presented as mean ± SD from 3 independent experiments unless otherwise indicated. Data were analyzed by 1-way analysis of variance, followed by Bonferroni post hoc tests in all cases. Significance was assigned at a p value ≤ 0.05.

Acknowledgements

We acknowledge the European Research Council for providing an ERC starting grant (309782) and the NWO for providing a VIDI grant (723.012.005) to F. J. Dekker.

Author contributions

TvdB performed histone acetylation experiments (blots and mass spectrometry) in RAW264.7 and PCLS, the gene expression in RAW264.7, the treatment of PCLS with compounds and wrote the manuscript; HW performed enzyme inhibition studies; NL prepared PCLS, and performed part of the gene expression in PCLS; PEW performed part of the gene expression in PCLS; JH assisted in mass spectrometry measurements; RB assisted in direction and design of the study, particularly regarding the mass spectrometry experiments; HJH assisted in direction and design of the study, particularly regarding the biological experiments; FJD conceived of the study, and assisted in its direction and in writing of the manuscript.

References

1. Keenan CR, Salem S, Fietz ER, Gualano RC, Stewart AG. Glucocorticoid-resistant asthma and novel anti-inflammatory drugs. Drug Discov Today 2012 Sep;17(17-18):1031-1038.
2. Telenga ED, Kerstjens HA, Postma DS, Ten Hacken NH, van den Berge M. Inhaled corticosteroids in chronic obstructive pulmonary disease: a review. Expert Opin Pharmacother 2010 Feb;11(3):405-421.
3. Babu KS, Kastelik JA, Morjaria JB. Inhaled corticosteroids in chronic obstructive pulmonary disease: a pro-con perspective. Br J Clin Pharmacol 2014 Aug;78(2):282-300.
4. Bird A. Perceptions of epigenetics. Nature 2007;447(7143):396-398.
5. Ganesan A. Multitarget Drugs: an Epigenetic Epiphany. ChemMedChem 2016 Jun 20;11(12):1227-1241.
6. Strahl BD, Allis CD. The language of covalent histone modifications. Nature 2000;403(6765):41-45.
7. Barnes PJ, Adcock IM, Ito K. Histone acetylation and deacetylation: importance in inflammatory lung diseases. Eur Respir J 2005 Mar;25(3):552-563.
8. Ito K, Caramori G, Lim S, Oates T, Chung KF, Barnes PJ, et al. Expression and activity of histone deacetylases in human asthmatic airways. Am J Respir Crit Care Med 2002 Aug 1;166(3):392-396.
9. Cosio BG, Mann B, Ito K, Jazrawi E, Barnes PJ, Chung KF, et al. Histone acetylase and deacetylase activity in alveolar macrophages and blood mononocytes in asthma. Am J Respir Crit Care Med 2004 Jul 15;170(2):141-147.
10. Su RC, Becker AB, Kozyrskyj AL, Hayglass KT. Altered epigenetic regulation and increasing severity of bronchial hyperresponsiveness in atopic asthmatic children. J Allergy Clin Immunol 2009 Nov;124(5):1116-1118.
11. Gunawardhana LP, Gibson PG, Simpson JL, Powell H, Baines KJ. Activity and expression of histone acetylases and deacetylases in inflammatory phenotypes of asthma. Clin Exp Allergy 2014 Jan;44(1):47-57.
12. Stefanowicz D, Lee JY, Lee K, Shaheen F, Koo HK, Booth S, et al. Elevated H3K18 acetylation in airway epithelial cells of asthmatic subjects. Respir Res 2015 Aug 5;16:95-015-0254-y.
13. Rajendrasozhan S, Yang SR, Kinnula VL, Rahman I. SIRT1, an antiinflammatory and antiaging protein, is decreased in lungs of patients with chronic obstructive pulmonary disease. Am J Respir Crit Care Med 2008 Apr 15;177(8):861-870.
14. Ito K, Ito M, Elliott WM, Cosio B, Caramori G, Kon OM, et al. Decreased histone deacetylase activity in chronic obstructive pulmonary disease. N Engl J Med 2005 May 12;352(19):1967-1976.
15. Hodge G, Jersmann H, Tran HB, Roscioli E, Holmes M, Reynolds PN, et al. Lymphocyte senescence in COPD is associated with decreased histone deacetylase 2 expression by pro-inflammatory lymphocytes. Respir Res 2015 Oct 24;16:130-015-0287-2.
16. Tan C, Xuan L, Cao S, Yu G, Hou Q, Wang H. Decreased Histone Deacetylase 2 (HDAC2) in Peripheral Blood Monocytes (PBMCs) of COPD Patients. PLoS One 2016 Jan 25;11(1):e0147380.
17. Dekker FJ, Haisma HJ. Histone acetyl transferases as emerging drug targets. Drug Discov Today 2009 Oct;14(19-20):942-948.
18. Dekker FJ, van den Bosch T, Martin NI. Small molecule inhibitors of histone acetyltransferases and deacetylases are potential drugs for inflammatory diseases. Drug Discov Today 2014 May;19(5):654-660.
19. Marmorstein R. Structure and function of histone acetyltransferases. Cell Mol Life Sci 2001 May;58(5-6):693-703.
20. van den Bosch T, Boichenko A, Leus NG, Ourailidou ME, Wapenaar H, Rotili D, et al. The histone acetyltransferase p300 inhibitor C646 reduces pro-inflammatory gene expression and inhibits histone deacetylases. Biochem Pharmacol 2016 Feb 15;102:130-140.
21. Morin JP, Baste JM, Gay A, Crochemore C, Corbiere C, Monteil C. Precision cut lung slices as an efficient tool for in vitro lung physio-pharmacotoxicology studies. Xenobiotica 2013 Jan;43(1):63-72.

22. de Kanter R, Monshouwer M, Meijer DK, Groothuis GM. Precision-cut organ slices as a tool to study toxicity and metabolism of xenobiotics with special reference to non-hepatic tissues. Curr Drug Metab 2002 Feb;3(1):39-59.
23. Legartova S, Stixova L, Strnad H, Kozubek S, Martinet N, Dekker FJ, et al. Basic nuclear processes affected by histone acetyltransferases and histone deacetylase inhibitors. Epigenomics 2013 Aug;5(4):379-396.
24. Cluntun AA, Huang H, Dai L, Liu X, Zhao Y, Locasale JW. The rate of glycolysis quantitatively mediates specific histone acetylation sites. Cancer Metab 2015 Sep 23;3:10-015-0135-3. eCollection 2015.
25. Zheng Y, Thomas PM, Kelleher NL. Measurement of acetylation turnover at distinct lysines in human histones identifies long-lived acetylation sites. Nat Commun 2013;4:2203.
26. Ghizzoni M, Haisma HJ, Maarsingh H, Dekker FJ. Histone acetyltransferases are crucial regulators in NF-κB mediated inflammation. Drug Discov Today 2011;16(11-12):504-511.
27. Oenema TA, Maarsingh H, Smit M, Groothuis GM, Meurs H, Gosens R. Bronchoconstriction Induces TGF-beta Release and Airway Remodelling in Guinea Pig Lung Slices. PLoS One 2013 Jun 26;8(6):e65580.
28. Eleftheriadis N, Neochoritis CG, Leus NG, van der Wouden PE, Domling A, Dekker FJ. Rational Development of a Potent 15-Lipoxygenase-1 Inhibitor with in Vitro and ex Vivo Anti-inflammatory Properties. J Med Chem 2015 Oct 8;58(19):7850-7862.

Supporting information

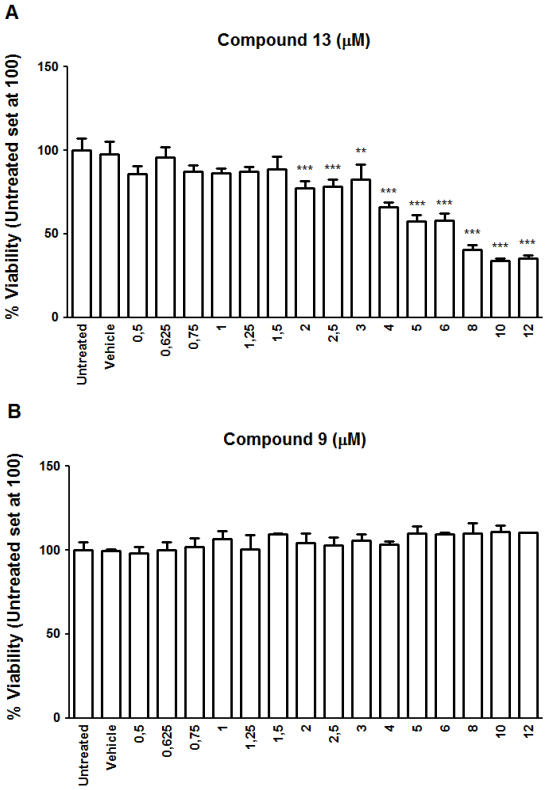

Figure S1. Results CellTiter 96 Aqueous One Solution Cell Proliferation Assay to determine viability of RAW264.7 upon **13** (A) or **9** (B) treatment. For the assay, cells were seeded at 7500 cells per well in 96 wells plates. On the following day, medium was replaced to medium containing **13** or **9** at the appropriate concentrations. After 20 hrs of incubation, the MTS reagent (Promega, Wisconsin, USA) was added to the wells. After one hr of incubation with this reagent, the absorbance at 490 nm was measured using a plate reader. The amount of absorbance at this wavelength is indicative of mitochondrial conversion of the MTS reagent, which in turn can be linked to cell viability. The experiment was done at least in triplicate. Compound **13** treatment reduced cell viability compared to vehicle treated cells from 2 µM and higher concentrations. *** $p < 0.001$ and ** $p < 0.01$ compared to vehicle (DMSO treated) cells. No statistical differences were observed between untreated cells, or cells treated with **9** at the indicated concentrations. Hence, we concluded that there is no cytotoxicity of **9** to RAW264.7 cells at these concentrations. Data are presented as mean values ± SD of 3-12 independent experiments.

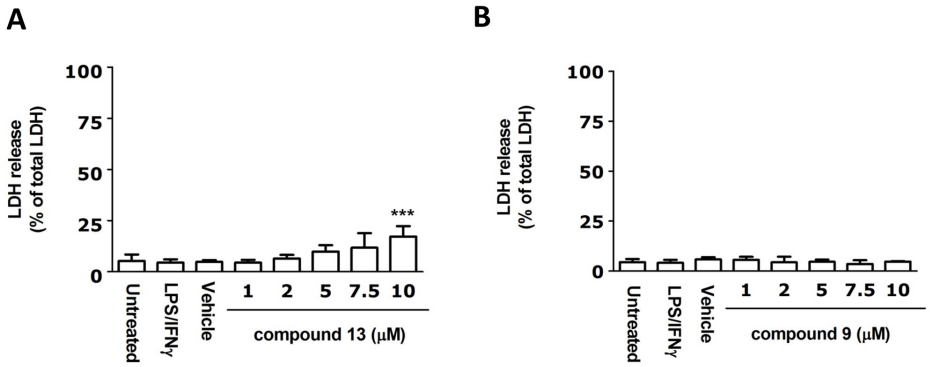

Figure S2. LDH assay results PCLS **13** (A) and **9** (B). To assess the viability of the PCLS subjected to **13** or **9** at the indicated concentrations, the amount of lactate dehydrogenase (LDH) released from the tissue slices into the incubation medium was analyzed. Maximal LDH release was determined by lysing 3 slices with 1% Triton X-100 for 30 min at 37°C at the start of the experiments. Supernatants were stored at -80°C. LDH release was determined using an assay form Roche Diagnostics (Mannheim, Germany), and was measured using a Hitachi automatic analyzer (Modular Analytics, Roche Diagnostics). LDH release from the PCLS into the incubation medium was plotted relative to maximal LDH release. Data are presented as mean values ± SD of 3 independent experiments.

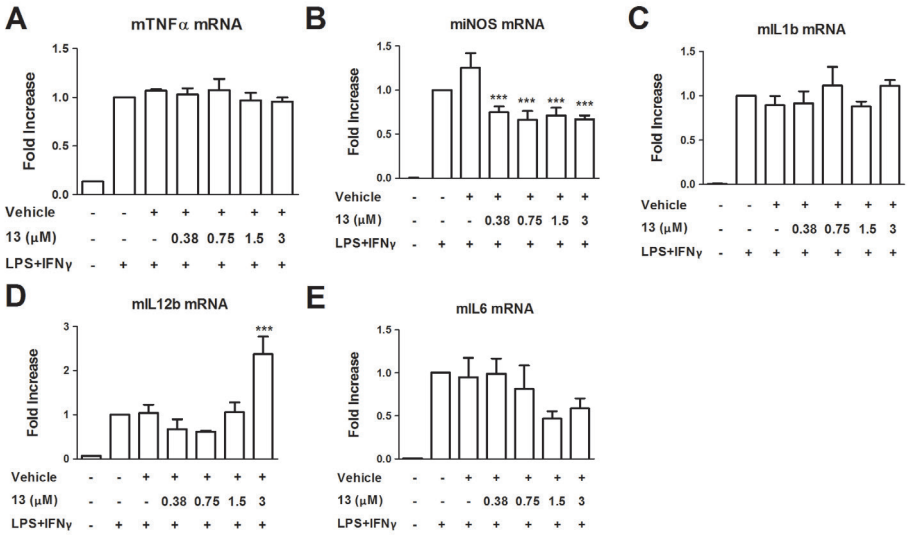

Figure S3. The effect of **13** treatment in RAW264.7 cells on the expression of A) *TNFα* B) *iNOS* C) *IL1β* D) *IL12b*, and E) *IL6*. RAW264.7 cells were pre-treated with **13** at the indicated concentrations for 16 hours, after which an inflammatory LPS and IFNγ stimulus (10 ng/mL of each) was given for 4 hours in continued presence of the inhibitor (total incubation time 20 hrs). Subsequently, gene expression was analyzed by RT-q-PCR. For vehicle treatment, RAW264.7 cells were pre-treated with the inhibitor solvent DMSO. Data represent the target gene expression normalized to the reference gene. The values shown are means ± SD of 3-4 independent experiments. *** $p < 0.001$ compared to vehicle.